ResearchHub JOURNAL

Structural Basis for Differential Affinity and Competitive Binding of DNA Polymerase Peptides to the Mycobacterial β-Clamp

Mavi Kapur[1], Olivia J. Gray[1], Shatabdi Sen[2], Richard B. Honzatko[1*], Scott W. Nelson[1*]

Published: May 4, 2025

[1] Roy. J. Carver Department of Biochemistry, Biophysics, and Molecular Biology, Iowa State University, Ames.
[2] Department of Plant Pathology, Iowa State University, Ames.

*Corresponding author: Scott W. Nelson, Roy J. Carver Department of Biochemistry, Biophysics and Molecular Biology, Iowa State University, 4112 Molecular Biology Building, Pammel Drive, Ames IA 50011-1079. Tel: 515-294-3434. Email: swn@iastate.edu

*Co-corresponding Author: Richard B. Honzatko, Roy J. Carver Department of Biochemistry, Biophysics and Molecular Biology, Iowa State University, 4206 Molecular Biology Building, Pammel Drive, Ames IA 50011-1079. Tel: 515-294-3434. Email: honzatko@iastate.edu

ABSTRACT

The β-clamp is a potential antibacterial target in mycobacteria and required for the processivity of the high-fidelity replicative polymerase DnaE1 during DNA replication. β-clamp also interacts with ImuB, which plays an important role in assembly of the low-fidelity DnaE2 mutasome. When DnaE1 stalls at DNA lesions, ImuB may facilitate its displacement from the β-clamp, allowing the DnaE2 mutasome to engage and replicate over the damaged DNA. Isothermal titration calorimetry indicates that specific sequences in ImuB significantly enhance its binding affinity to the β-clamp as compared to DnaE1. Both crystallographic and molecular dynamics analyses support a common binding site and conformation for these interactions, suggesting a competitive mechanism that is essential for adapting to genotoxic stress. This interaction highlights the β-clamp's dual role in genome stability and adaptability, positioning it as a strategic target for therapies that simultaneously block DNA replication and mutagenesis in mycobacteria.

Keywords: Mycobacterium, mutagenesis, motifs, peptide

Key Messages:

1. **Differential Affinity Drives Polymerase Switching at the β-Clamp**
   This study reveals that the ImuB peptide binds to the mycobacterial β-clamp with ~40-fold greater affinity than the DnaE1 replicative polymerase peptide, a difference primarily driven by optimal sidechain packing at residue 2 (Leu vs. Phe). Crystal structures and molecular dynamics simulations show that both peptides adopt similar binding conformations, but the ImuB motif is pre-organized for binding, reducing entropic penalties. This affinity advantage supports a model where ImuB competitively displaces DnaE1 at DNA lesions, enabling a switch from high-fidelity to low-fidelity replication under genotoxic stress.

2. **The β-Clamp as a Dual-Function Drug Target**
   The β-clamp serves as a central hub in both DNA replication fidelity and adaptive mutagenesis. By interacting with both DnaE1 and ImuB through a conserved binding site, it facilitates polymerase switching. This shared interface presents a promising antimicrobial target: inhibitors blocking this site may simultaneously suppress replication and prevent mutagenic adaptation, offering a strategy to counteract drug resistance in tuberculosis.

INTRODUCTION

Tuberculosis (TB), caused by the bacterium *Mycobacterium tuberculosis*, damages primarily lung tissue, but can also spread to other parts of the body[1]. Despite drug therapy and a neonatal vaccine, TB is a leading cause of death worldwide. Most deaths are due to drug-resistant forms of TB, the existence of which underscores the need for new therapies[2].

Given the critical role of DNA replication machinery in bacterial survival and replication, targeting this system offers a promising strategy for developing new antibacterial agents. Proteins such as the β-clamp, a ring-shaped homodimeric protein that enhances the processivity of DNA polymerase III, are essential for bacterial DNA replication. The β-clamp not only interacts with DNA polymerase III but also with other proteins involved in replication and repair, helping to maintain genomic integrity under various stress conditions[3,4]. This makes it a particularly attractive target for novel drug development, as its inhibition could disrupt the entire process of DNA replication, leading to bacterial cell death.

While β-clamp interactions with Escherichia coli DNA polymerases and other replication proteins have been well studied[5–7], how this knowledge translates to mycobacteria remains unclear. In Mycobacteria, multiple DNA polymerases interact with the β-clamp, but the mechanisms that determine how they compete for binding to β-clamp, especially between the high-fidelity polymerase DnaE1 and ImuB, a central component of the low-fidelity DnaE2 mutasome, are not well understood.

To facilitate biochemical and structural characterization of these mycobacterial interactions, we employed the β-clamp from the thermophilic homolog *Mycobacterium thermoresistibile*. Proteins from thermophiles typically display enhanced stability and solubility, greatly simplifying heterologous protein expression and purification, and this choice is particularly advantageous because several components of the DnaE2 mutasome are notoriously difficult to isolate.

DnaE1, the replicative polymerase responsible for copying the mycobacterial genome, belongs to the Pol-C family of polymerases that contain polymerase, PHP and oligonucleotide binding domains[8]. DnaE1 replicates DNA with high-fidelity and contains a proofreading activity that is housed in the PHP domain[9–11]. During genomic replication DnaE1 combines with clamp loader and β-clamp to form the DNA Pol III holoenzyme. Interaction of DnaE1 with β-clamp is through a QFDLFG sequence motif[12].

ImuB is one of the key proteins employed by mycobacteria for damage tolerance and mutagenesis. It appears to share all structural features of Y-family polymerases but lacks polymerase activity and conserved catalytic residues. ImuB appears to be a scaffold protein, interacting with all the other metasoma components. ImuB interacts with β-clamp via a QLPLWG sequence motif[13].

The aforementioned sequence motifs are hypothetically responsible for binding interactions between β-clamp and mycobacteria polymerases. Conceivably, the ImuB motif has the highest affinity for β-clamp relative to sequence elements of other polymerases. Hence, upon induction in response to DNA damage, ImuB will enable the low-fidelity DnaE2 polymerase to displace the high-fidelity polymerase.

In this work, the interactions of peptides with β-clamp were analyzed by isothermal titration calorimetry (ITC) and X-ray crystallography. Experiments reveal a higher binding affinity for the ImuB peptide relative to that of the DnaE peptide. Crystal structures of β-clamp-peptide complexes are consistent with the findings of ITC. The ImuB peptide β-clamp structure reveals more hydrogen bonds and hydrophobic interactions relative to DnaE1-peptide complex structure. Molecular dynamics (MD) simulations and principal component analysis (PCA) revealed a single, tightly focused cluster of conformations for the LPL residues of the ImuB peptide in solution that matches the bound conformation. Other peptides have multiple, unfocused clusters. Interestingly, the LPL-motif is also present in grislemycin, a natural inhibitor of the β-clamp[12,14].

The low dissociation constant (K_d) value for the β-clamp complex with ImuB-peptide, the comparable binding affinities of ImuB-peptide and the truncated N-terminal half of ImuB, and the existence of the LPL-motif in a potent natural inhibitor suggest a preference for the association of β-clamp and ImuB in vivo. A small molecule to be effective as a drug must have a K_d significantly lower than the ImuB-peptide. Success in the displacement of the high-fidelity polymerase, coupled with the failure to displace the low-fidelity polymerase, would lead to a rapidly mutating organism, more likely to escape the benefits of current drug therapies.

METHODS

Protein Expression and Purification: The open reading frame for β-clamp from *Mycobacterium thermoresistibile*, codon-optimized for expression in E. coli, was cloned into the pSUMO vector. E. coli BL21 were transformed for recombinant protein expression and grown at 37 ºC with shaking and with 30 µg/ml kanamycin. IPTG was added to a concentration of 0.2 mM after cell cultures reached OD600 nm to 0.6-0.8. Subsequently, cultures were maintained at 16 ºC with shaking for 18 hrs. Cells were lysed using a homogenizer and a β-clamp construct having a Sumo-His6 tag at the N-terminus was purified using Ni-NTA agarose and size-exclusion Superdex-200 columns. The Sumo-His6 tag was cleaved by sumo protease in a low-salt buffer (20 mM Tris, and 50 mM NaCl, pH 8). Tagged components were removed by the passage of the proteolyzed construct through a Ni-NTA agarose column. Purified protein was analyzed by SEC-MALS, resulting in the expected molecular mass for a dimer (84 kDa). Protein in 20 mM Tris and 50 mM NaCl, pH 8, was concentrated to 14 mg/ml for subsequent experimental work.

ImuB was purified similarly to β-clamp by Ni-NTA agarose and size exclusion chromatography. Purified full-length ImuB was unstable in the absence of arginine (200 mM, pH 8.0). Based on sequence and structural similarity to Y-family DNA polymerases, it was hypothesized that residues 395-422 of ImuB may promote self-aggregation. Truncation of the C-terminus of ImuB, retaining residues 1-361 and the β-clamp binding motif, provided a stable protein construct (Tr-ImuB), isolated by the same protocol as ImuB. Tr-ImuB analyzed with SEC-MALS was monomeric with an observed molecular mass of 38 kDa.

Crystallography of Ligand-Free β-Clamp: Initial screens using a Mosquito crystallization robot resulted in crystals under 20 different conditions. All exhibited only low-resolution x-ray diffraction due to inadequate cryoprotection. Subsequently, crystals grown by combining equal volumes of β-clamp (14 mg/ml in 20 mM Tris and 50 mM NaCl, pH 8) and precipitant solution (4 M ammonium acetate, 0.1 M bis-tris propane pH 7 and 8% glycerol by the method of hanging drop, diffracted to 3.2 Å at ALS Berkeley on beamline 4.2.2. The crystal structure of the *M. thermoresistibile* β-clamp was solved by molecular replacement using the model for *M. tuberculosis* β-clamp (PDB ID: 3P16)[15]. Refinement employed Phenix/Coot[16] and incorporated donor-acceptor restraints to enforce ideal geometry in regions of regular secondary structure.

Crystallography of β-Clamp with Peptides: Sequences of β-clamp binding motifs in the Mycobacterial DnaE1 and ImuB proteins are QFDLFG and QLPLWG, respectively. Peptides came from Genscript with acetyl (Ace) and amide groups at their N- and C-termini, respectively. Solutions of β-clamp (14 mg/ml in 20 mM Tris and 50 mM NaCl, pH 8) saturated with the peptide were combined with an equal volume of precipitant screening solutions using a Mosquito robot. Crystals of β-clamp with DnaE1-peptide formed in 0.5 M ammonium sulfate, 0.1 M sodium acetate, pH 5.6 and diffracted to 2.8 Å. β-clamp with ImuB-peptide crystallized from 60% tascimate pH 7, 0.1 M Bis-Tris pH 6.3 and showed diffraction to 2.5 Å. Crystals were dipped in 5 and 10% glycerol for cryoprotection prior to freezing in liquid nitrogen. Data were collected at Argonne National Laboratory, APS beamline 23ID-D. Structures were solved by molecular replacement using the ligand-free β-clamp from *M. thermoresistibile* (this work, PDBID: 8DKD). Refinement employed Phenix/Coot, and incorporated donor-acceptor restraints to enforce ideal geometry in regions of regular secondary structure.

Isothermal Titration Calorimetry (ITC): Titrations employed a Malvern Microcal ITC-200. Peptides from 1-2.5 mM were titrated into 65-100 μM β-clamp in 20 mM Tris and 50 mM NaCl, pH 8. Titrations using the DnaE1-peptide included 5% DMSO to increase the solubility of the peptide. Used as a titrant, Tr-ImuB (20mM) was in 20 mM Tris and 200 mM NaCl, pH 8. All the reactions were carried out at 25ºC and stirred at 500 rpm. Data were analyzed using several binding models with Origin software provided with the instrument. When the stoichiometry (n) of the reaction was an adjustable parameter, the n values were near unity in all cases (1.1 to 0.9). In order to facilitate a direct and more accurate comparison of K_d values, n was fixed to 1.0 per clamp subunit, as indicated by the x-ray crystal structures.

Molecular Dynamic Simulations: The GROMACS program suite and the OPLS-AA force field were used in the simulations for the free peptides[17]. Each peptide was solvated in a cubic box of SPC water, keeping a minimum distance of 10 Å between the solute and each face of the box. The equation of motion was integrated by using a leapfrog algorithm with a time step of 2 fs. Covalent bond lengths were constrained by the procedure LINCS (LINear Constraint Solver) with lincs-order of 4 and lincs-iter of 1. A twin-range cutoff of 1.0/1.0 nm was used for the nonbonded interactions. The nonbonded interaction pair-list was updated every 20 fs. The solute and solvent were separately weakly coupled to external temperature baths at 300 K. The temperature-coupling constant was 0.1 ps. The total system was also weakly coupled to an external pressure bath at 1 atm using a coupling constant of 2.0 ps.

Starting with a fully extended configuration of the peptide, the equilibration protocol consisted of 50000 steps of steepest-descent minimization applied to the solvent molecules with fixed solute, followed by 5000 ps of MD simulation at 300 K of the solvent with fixed peptide, and another 5000 ps simulation without position constraining of peptide sequence. The simulation was then continued for 1000 ns, whereby the coordinates were saved every 1.0 ns for analysis. Following the MD simulation, for the identification of kinetically relevant states and their interconversion rates from the simulated trajectories, PyEMMA was used to construct and analyze the MSM from all the obtained trajectories[18].

RESULTS

Isothermal Titration Calorimetry (ITC)

The changes in enthalpy (ΔH), entropy (ΔS), free energy (ΔG), and the resulting K_d were obtained from ITC. The K_d values for complex formation of β-clamp with ImuB and DnaE1 motifs and Tr-ImuB were 0.93, 37.2, and 0.73 μM respectively (Table 1).

Table 1. Thermodynamic Parameters from ITC for β-clamp interactions with peptides and Tr-ImuB.

Protein	**K_d ± SE (μM)**	**ΔH ± SE (kcal/mol)**	**ΔG ± SE (kcal/mol)**	**ΔS ± SE (kcal/mol/K) x 1000**
ImuB peptide (QLPLWG)	0.9 ± 0.1	-11.1 ± 0.2	-8.23 ± 0.06	-9.6 ± 0.7
DnaE1 peptide (QFDLFG)	37 ± 1	-6.8 ± 0.3	-6.04 ± 0.02	-2.6 ± 1
Tr-ImuB	0.73 ± 0.09	-13.5 ± 0.1	-8.37 ± 0.07	-17.2 ± 0.3
ImuB position 3 P to D peptide (QLDLWG)	2.2 ± 0.4	-8.2 ± 0.7	-7.7 ± 0.1	-1.7 ± 2
DnaE1 position 3 D to P peptide (QFPLFG)	22 ± 1	-5.9 ± 0.3	-6.33 ± 0.03	1.4 ± 1

ImuB-peptide and Tr-ImuB have similar binding constants, suggesting only the ImuB motif of Tr-ImuB contributes to affinity and that Tr-ImuB binds in a similar manner as ImuB peptide motif. Therefore, we hypothesize that Tr-ImuB is interacting with β-clamp with only QLPLWG motif and secondary interactions, if present, are negligible. Our results demonstrate that ImuB peptide has a 40-fold higher affinity as compared to the DnaE1 motif, suggesting that upon induction of ImuB, it will out-compete the replicative polymerase during DNA damage and thus favor mutagenesis. Analysis of the ITC data also indicates that the binding reactions are primarily exothermic, and the heat evolved can be the result of H-bond formation between the peptides and β-clamp (Figure 1).

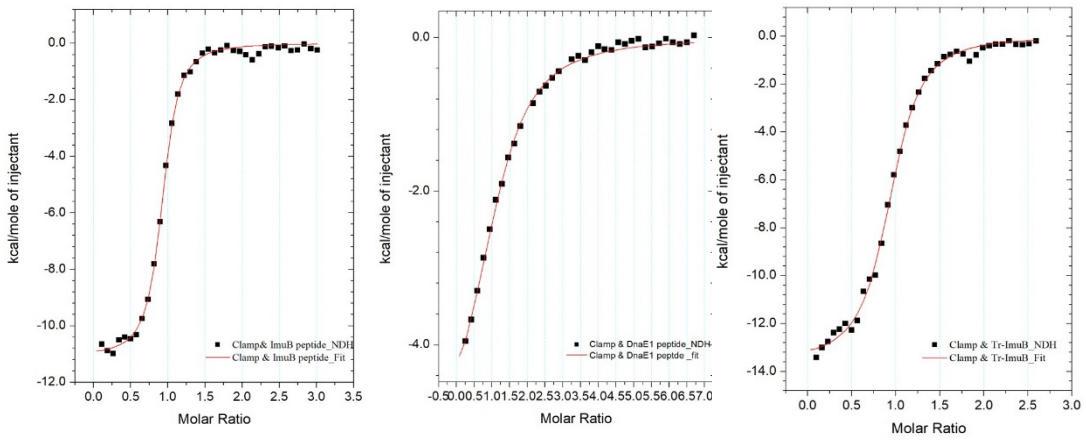

Figure 1. ITC of the interaction of β-clamp and ImuB peptide, DnaE1 peptide and Tr-ImuB at pH 8 at 25°C

Crystallography

Statistics of data collection and refinement are in Table 2. Crystals of β-Clamp in complex with ImuB-peptide and DnaE1-peptide clearly revealed electron density for peptides in Fo-Fc electron density maps using phases from molecular replacement.

Table 2. Statistics of data collection and refinement for structure of β-clamp from *M. thermoresistibile*. Coordinates and structure factors were deposited in PDB.

β-Clamp complex	Ligand-free PDBID:8DKD	ImuB-QLPLWG Peptide PDBID:8DJ6	DnaE1- QFDLFG Peptide PDBID:8DJQ
Space group	P 31 2 1	C 1 2 1	P 1 21 1
Unit cell parameters	*a*=102.408 Å *b*=102.408 Å *c*=34.159 Å α=90° β=90° Y=120°	*a* = 214.110 Å *b* = 124.832 Å *c* = 117.262 Å α = 90° β = 113.75° γ = 90°	*a* = 66.81 Å *b* = 148.252 Å *c* = 81.952 Å α = 90° β = 92.183° γ = 90°
No. of images (step/image in degrees)	900 (0.2)	895(0.2)	900(0.2)
No. of observations	107,109	1369270	839055

No. of unique reflections	12,957	94384	38930
Resolution range (Å)	45-3.2	19.89-2.5	19.98-2.80
Completeness of data (%)			
Overall	92.9	96.4	99.52
Last shell (Å)	32.6 (3.32-3.2)	89 (2.54-2.50)	99 (2.85-2.80)
CC1/2			
Overall	0.991	0.964	0.967
Last shell (Å)	0.595 (3.32-3.2)	0.756 (2.54-2.50)	0.421(2.85-2.80)
R-merge			
Overall	0.057	0.123	0.153
Last shell (Å)	0.679 (3.32-3.2)	0.988(2.54-2.50)	0.471(2.85-2.80)
No. of reflections used in refinement	12,943	94,256	38,932
No. of atoms (H-included)	5939	24034	24140
No. of non-hydrogen atoms	2963	12155	12265
Solvent atoms	55	371	504
Average B ($Å^2$)	129	64.15	62.21
R-work			
Overall	0.25	0.20	0.22
Last shell (Å)	0.366 (3.32-3.2)	0.29 (2.56-2.50)	0.36
R-free			
Overall	0.279	0.22	0.28
Last shell (3.32-3.2 Å)	0.389 (3.32-3.2)	0.32 (2.56-2.50)	0.47 (2.9-2.80)
Parameters of stereochemistry			
No. of donor-acceptor restraints	205	816	891
Bonds (rmsd in Å)	0.004	0.0015	0.0013
Angles (rmsd in °)	0.681	0.53	0.52
Ramachandran outliers (%)	0	0	0
Ramachandran favored (%)	91.9	96.03	94.70
Rotamer outliers (%)	1.3	0.24	0.24
Clash score	0.57	0.38	0.55
Molprobity score	1.24	0.91	1.04

Crystal structures and light scattering (SEC-MALs) experiments exhibited β-clamp to be a homodimeric protein of molecular mass 84 kDa. The asymmetric unit for the non-ligated β-clamp (space group $P3_121$) has a single polypeptide chain (Chain A); the symmetry axis of the biological dimer coincides with the crystallographic twofold axis. The peptide complexes each have four polypeptide chains in their asymmetric units (Chains A, B, C and D and four peptide molecules (Chains E, F, G and H, associated with Chains A, B, C and D, respectively). For the peptide complexes, Chains A and C (also Chains B and D) define a biological homodimer.

The model for the polypeptide chain in the non-ligated β-clamp is in continuous electron density from residues 9-397. For the 12 polypeptide chains of the peptide complexes, the first observed residue of polypeptide chains varied from 2 to 9 and the last observed residue ranged

from 396 to 397. For the DnaE1-peptide complex, residues 229-235 were omitted from the all the peptide chains, otherwise density was present to model the main chain, albeit some side chains are in weak or noise-level electron density.

M. thermoresistibile was chosen as the model system for this study because proteins derived from thermophilic organisms generally demonstrate improved stability and solubility, facilitating easier expression and purification compared to mesophilic counterparts[19]. Even though β-clamp from Mycobacterium species exhibits robust expression, other components of the Mycobacterium mutasome (e.g., DnaE2 and ImuB[13]) have proven to be very difficult to express and purify in *E. coli*, and our ultimate goal is to characterize the structure and function of the entire mutasome. Thermophilic proteins tend to have more hydrophobic clusters, H-bonds, salt bridges, and cation-π interactions, which are thought to contribute to their increased stability compared to their mesophilic counterparts[20,21] Comparative analysis of all these interactions revealed that β-clamp from *M. thermoresistibile* has approximately the same number of hydrophobic clusters, more salt bridges (33 *vs.* 21) and H-bonds (51 *vs.* 43) than *M. tuberculosis* clamp, but less cation-π interactions (4 *vs.* 5)[22–24]. These differences are minor, and it is unclear if these additional interactions have a significant impact on thermostability. Overall, the non-ligated β-clamp from *M. thermoresistibile* is comparable in structure to that of *M. tuberculosis* (overall rmsd deviation in main chain atoms of 1.24 Å). Each subunit has three domains, I, II and III (Figure 2) I (residues 1-126) II (residues127-262) and III (residues 267-397). Each domain puts two alpha-helices at the inside surface of the ring. These helices pack against β-sheets that in turn define the outside surface of the ring. The β-clamp annulus has a positive charge on the inside surface that supports probable interactions with DNA. Interactions between domains I and III of different subunits stabilize a ring-shaped biological dimer. The dimer interface appears to be stabilized by hydrophobic as well as ionic interaction between a glutamate side-chain of one domain and an arginine side-chain from the other. β-strands at the edges of the β-sheets in Domain I & III anneal with each other to further support the dimeric assembly.

Residues 216--222 and 230--238 (C-terminal regions of each helix of Domain II) exhibit significant structural variation amongst the 13 independent polypeptide chains reported here. The variations are due to weak or absent electron density, but may reflect structural elements, predisposed to conformational change in the movement of the β-clamp along ds-DNA.

β-Clamp-Peptide Complexes

Structures of the peptide complexes reveal that the peptides bind to the same site, one to each subunit of the β-clamp. β-clamp has hydrophobic pocket formed by the two subsites (1,2) connected by shallow groove. Subsite-I is formed by residues L184, L162, T179, R181, P257, L262, L389 and P360 whereas subsite-II has N334, Y337, S358, M391, P392, V393 and R394. The first three residues of the peptide are interacting in subsite-2 while remaining residues interact with subsite-1 (Figure 3A, S1A). Each of the three β-clamp-peptide complexes superimpose onto apo-β-clamp with an average RMSD of 1.1 Å. There is a difference of 0.5-1 Å in the position of residues at some locations (Figure 3B). Three donor-acceptor interactions involving elements of the main chain and functional groups of the peptide are common to the three complexes (Table 3, Figure S1B).

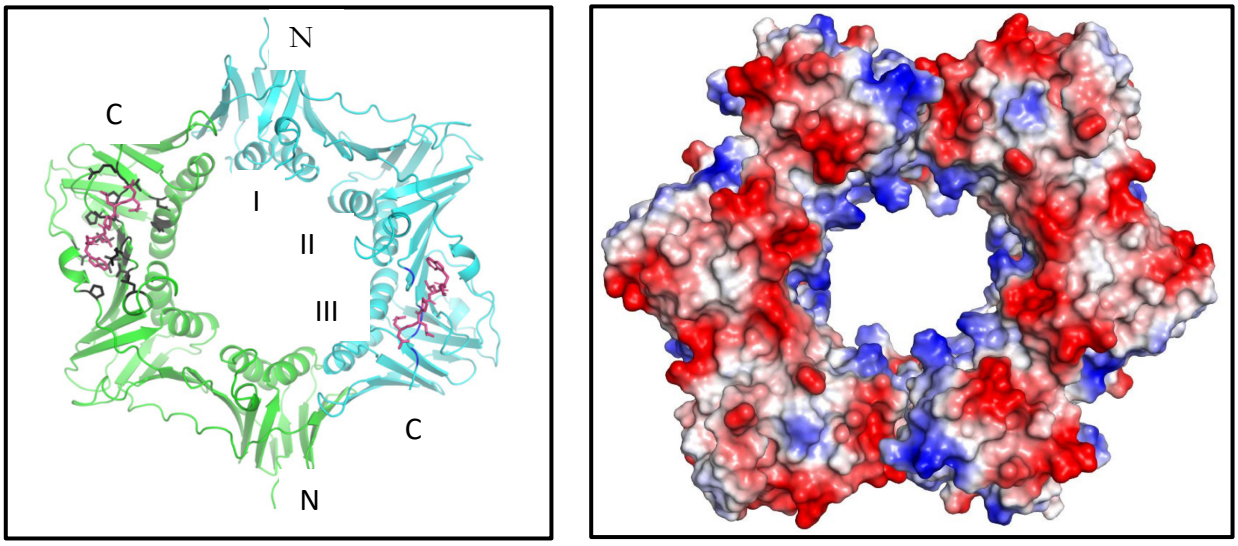

Figure 2. A) Ribbon representation of the ring-structure of the *M. thermoresistible* clamp-peptide complex where clamp monomers are shown in green and cyan and peptide is shown in pink. Domains of one subunit are labeled by Roman numerals. B) Surface potential map of the clamp dimer. Red represents negatively charged residues, grey represents neutral residues and blue represents positively charged residues. Central hole accommodates double stranded DNA.

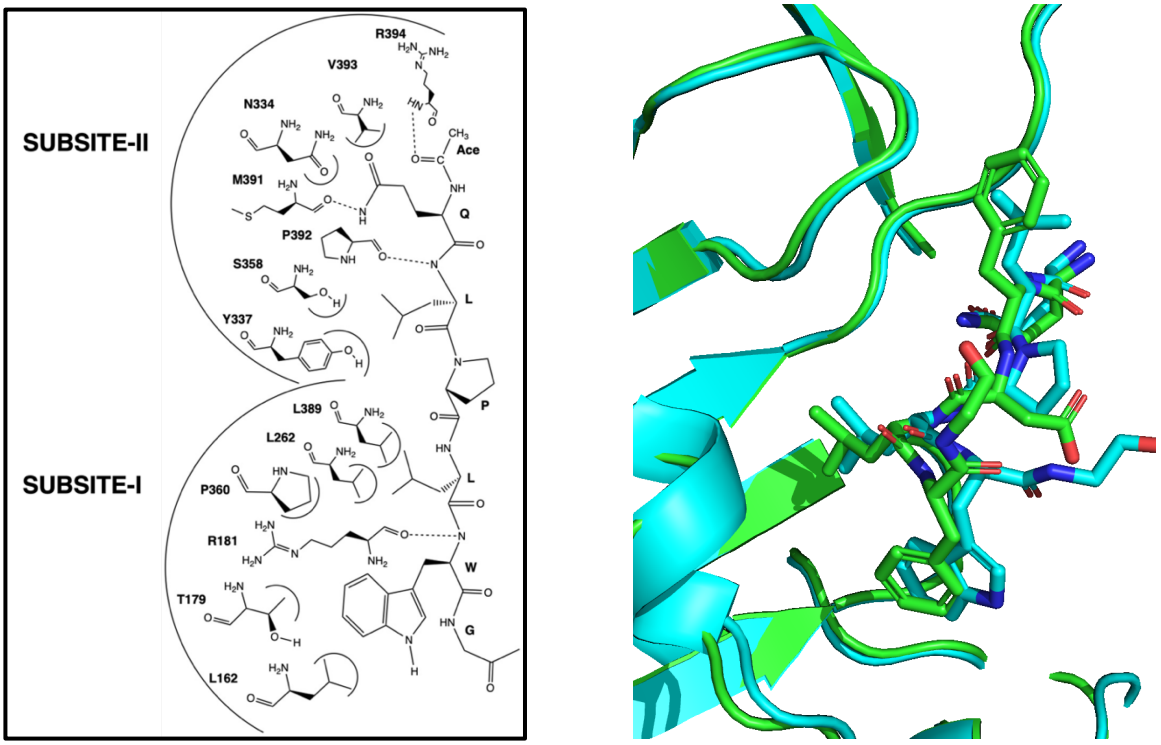

Figure 3. A) Schematic of interactions of the sliding clamp and ImuB peptide in the subsite-I and II. B) Chain E superimposed from all the clamp peptide complexes (ImuB peptide in cyan and DnaE1 in green).

Interactions in the β-Clamp-ImuB Peptide Structure

Interactions in subsite II: As mentioned above, residues (Ace, Q and L) are interacting in the subsite-2 of the hydrophobic pocket. The N-acetyl group is interacting by forming an H-bond with the amine 'N' of R394. Q2 is making multiple interactions with the protein, its backbone is making a hydrophobic interaction with V393, whereas side chain NE2 of glutamine is forming a H-bond with carbonyl 'O' of the M391. The NE2 of Q2' is also forming an internal H-bond with the carbonyl oxygen of L3'. Main chain N of the amine of L3' is forming a H-bond with carbonyl group of P392 whereas sidechain of leucine is interacting hydrophobically with S358 and M391 and R394 sidechain (Figure 3A and Figure S1A&B).

Proline is located between the two subsites and is not directly interacting with the clamp. Proline is a sterically constrained amino acid, so it could restrict the conformation of the free peptide, thereby favoring complex formation. To investigate this further, MD simulations were performed on free and bound peptide and Ramachandran coordinates were depicted, which will be presented in the later section.

Interactions in subsite II: Carbonyl oxygen of the R181 is making a H-bond with the amine 'N' of the L-5 whereas its side chain is fitting in the hydrophobic pocket formed by T179, L184, L262, L389 and P360. R181 is making a second interaction with peptide by forming an H-bond between its side chain and carbonyl O of W6' (Figure S1B). The aromatic ring of tryptophan provides a hydrophobic interaction with the residues M161, L162, T179 and P257 in the subsite (Figure S1A).

Common interactions among the peptide structures. Both peptides have an N-acetyl group, a Q, and an L in positions 1, 2 and 5, and they are making identical interactions in all the structures. Table 3 illustrates the β-clamp residues that are interacting with peptide residues and average length of H-bond between them.

Table 3. Donor acceptor interactions common to β-clamp-peptide complexes. The distances are averages and standard errors are based on four chain-peptide complexes of each asymmetric unit.

Peptide residue/position	β-clamp	Donor-acceptor distance (Å) ImuB-peptide	Donor-acceptor distance (Å) DnaE1-peptide
Backbone carbonyl, N-Acetyl1'	Backbone amide, R394	2.75 ± 0.04	2.75 ± 0.02
Sidechain, Q2 (NE2)	Backbone carbonyl, M391	2.86	2.95 ± 0.06
Backbone amide, position 3	Backbone carbonyl, P392	2.86	3.18 ± 0.1
Backbone amide, L5	Backbone carbonyl, R181	2.76 ± 0.04	2.99 ± 0.05

Differences Between the ImuB and DnaE1 Peptides

β-clamp and DnaE1: In this structure, we were able to map initial N and C-terminal residues of β-clamp that were not observed in published structures. As compared to ImuB peptide, there is no

additional H-bond between the sidechain of R181 and the backbone amide of position-6 (Figure S1B and S2B). However, the DnaE1 peptide forms an H-bond between the backbone amide of position-3 and the carbonyl of P392, although it appears to be weak with an average length of 3.18 Å (Figure S1B and S2B). In one of the four peptides, the sidechain of aspartate at position 4 is in different conformation, which has resulted in the establishment of an internal H-bond between the side chain of D4 and L5. As compared to ImuB peptide, the DnaE1 peptide has fewer interactions, suggesting weaker binding to β-clamp.

Conformation of Peptides in Solution and Bound to β-Clamp

Molecular dynamics simulations revealed conformational variation and preferred conformational state of each peptide. Principal component analysis revealed a single conformation in solution for the ImuB peptide and multiple conformational states for the DnaE1 peptide. The phi and psi angles of residue 3 of the DnaE1 peptide (Asp) reveal as many as four preferred combinations of mainchain angles, whereas phi and psi angle for the Pro 3 of the ImuB-peptide has only a single preferred state (Figure 4). While all peptides could achieve the conformation of the bound state, the only allowed conformation of ImuB peptide is identical to that of its bound conformation.

Analysis of Position 3 of the β-Clamp Binding Motif

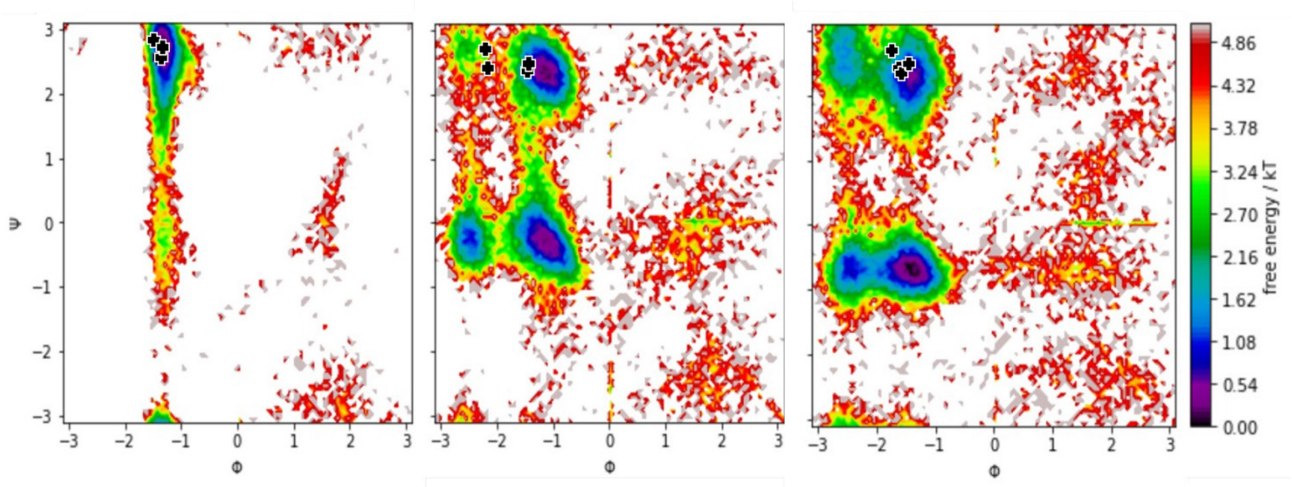

Figure 1. Ramachandran Plot and free energy plot generated for Proline, Serine and Aspartate residues from the MD simulations and coordinates of the bound peptide from complexes are superimposed as black (+) signs.

We hypothesized that the increased binding affinity of the ImuB peptide was due either to more optimal contacts between the β-clamp and the leucine residue at position 2 or to the restricted conformation of the peptide caused by the proline substitution at position 3. To investigate each possibility, we conducted ITC experiments and performed MD simulations on peptides with various mutations at position 3. The MD simulations of the mutant peptides (ImuB position 3 P→D and DnaE1 position 3 D→P) confirmed that the presence or absence of a proline residue at position 3 was sufficient to either restrict or allow, respectively, conformational heterogeneity of the peptide (Figure 5).

If the increased binding affinity of the ImuB peptide were primarily due to the restricted conformation of the unbound peptide, we would expect the K_d value for ImuB position 3 P→D to be similar to those of the wild-type DnaE1 peptides, while the K_d value for DnaE1 position 3 D→P should approach that of the wild-type ImuB peptide. The ITC binding data of the mutant peptides indicated that this is not the case (Table 1, Figure S3). Specifically, the binding affinity for the ImuB position 3 P→D peptide was only modestly weaker (~2.4-fold) compared to the wild-type ImuB peptide, and the K_d value for the DnaE1 position 3 D→P peptide was largely unchanged compared to the wild-type sequences. These observations indicate that while conformational restriction contributes to binding affinity, it alone cannot account for the full magnitude (~40-fold) of the observed affinity difference between the wild-type peptides.

Given the modest affinity differences attributable to residue 3, we turned our attention to the substantial enthalpic differences between peptides containing leucine or phenylalanine at position 2. ITC data revealed an enthalpy difference of approximately 5 kcal/mol between these peptides, suggesting substantial changes in sidechain packing and intermolecular interactions. Structural analyses of the peptide–β-clamp complexes support the conclusion that optimal sidechain packing and interactions at residue 2 significantly contribute to the high binding affinity observed for the ImuB peptide. Thus, we conclude that differences at residue 2 constitute the primary determinant of the differential binding affinity, with residue 3 providing a secondary, though still relevant, contribution through its influence on peptide conformation.

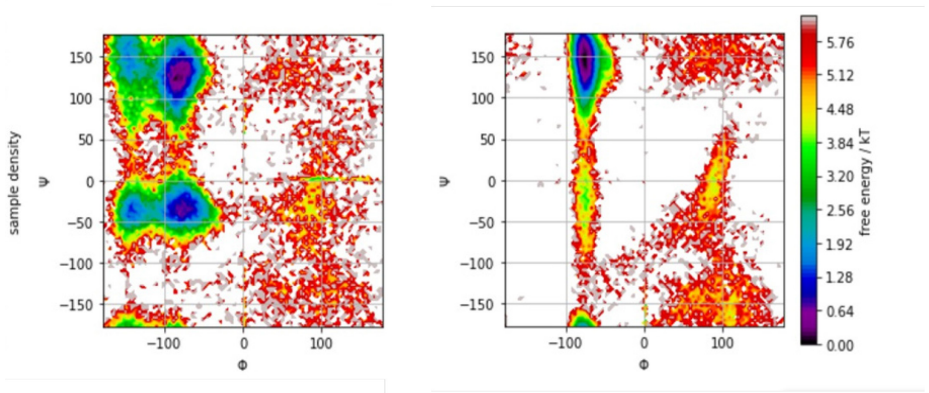

Figure 5. Ramachandran and free energy plots generated from the MD simulations of the Aspartate (left) and Proline (right) residues of the ImuB position 3 P→D and DnaE1 position 3 D→P peptides, respectively.

DISCUSSION

M. thermoresistibile has only a single clamp protein that must recognize multiple DNA polymerases[25,26]. A motif of five residues is the only known element recognized by the β-clamp[27], and in the case of ImuB, data here support the five-residue motif as the sole determinant of binding affinity as ImuB peptide and truncated ImuB have the same binding affinities within experimental uncertainty. Additionally, DnaE1- and ImuB-peptides bind to the same site on β-clamp and adopt similar bound conformations in crystal structures. These structural and thermodynamic data are consistent with a common mechanism and mode of binding to the same site of the clamp.

Investigations of other clamp-peptide complexes have demonstrated the importance of glutamine as the first amino acid of the peptide motif[27]. In the DnaE1- and ImuB-peptide complexes of the clamp from *M. thermoresistibile*, the sidechain of glutamine displaces a water molecule, replacing hydrogen bonds of the water molecule with those of the sidechain. Similarly, crystal structures indicate a precise fit of the leucyl sidechain (at position 4 of both peptides) in a hydrophobic pocket that would not tolerate different amino-acid sidechains without loss of binding affinity. Although position 5 (Phe or Trp) and position 6 (Ala or Gly) vary, these sidechains appear not to interact as strongly with the β-clamp in crystal structures. Hence, we consider variations in positions 2 and 3 of the peptides as being the primary cause for different peptide affinities.

The favorable free energy of binding exhibited by the ImuB peptide relative to the DnaE1 peptide may be due in part to the conformation of each peptide in solution. Molecular dynamics simulations reveal multiple conformations of peptides in solution when position 3 is aspartate, whereas only one conformational state exists when position 3 is proline. Moreover, when position 3 is proline, the peptide conformation corresponds closely to the clamp-bound conformational state (Figure 4). Hence, for the ImuB peptide with position 3 as proline there is a smaller entropic penalty in going from multiple conformations in solution to a single bound conformational state. The effect on peptide-binding affinity, however, appears modest; QLPLWG binds 2- to 3-fold more tightly than QLDLWG. Proline at position 3 alone cannot be responsible for the tight binding of the ImuB peptide to the clamp.

The DnaE1 peptides with position 2 as phenylalanine have K_d values ranging from 22 to 37 □M, whereas peptides with position 2 as leucine have K_d values from 0.9 to 2.2. Therefore, the data support position 2 as the primary basis for differences in the binding affinities between DnaE1- and ImuB-peptides, with a secondary role for proline at position 3. The differences in the enthalpy of binding for leucine vs. phenylalanine (5 kcal/mol) is large and unlikely due to nonbonded contacts alone between the sidechain and clamp protein. (For instance, the loss of a buried carbon or oxygen atom causes a ~2 kcal/mol increase in enthalpy). Instead, we suggest leucine at position 2 provides an optimal fit to a hydrophobic pocket while simultaneously facilitating optimal fits at position 1 (glutamine) and position 4 (leucine). The phenylalanine at position 2 compromise sidechain interactions at positions 1 and 4. High-affinity binding then is due to optimal interactions of QLPL, and substitutions of any of these residues weakens affinity. Interestingly, grislemycin, a natural inhibitor has two LPL motifs in a constrained cyclic peptide and exhibits the highest known affinity of a small peptide for a β-clamp[14].

The binding affinities of ImuB- and DnaE1-peptides may improve when each is part of a larger protein. Conformational restraints due to covalent linkages at the N- and C-termini of each peptide may limit conformational variation. Nonetheless, provided that the binding affinities of the parent proteins are represented faithfully by the binding affinities of their peptides, then ImuB should displace DnaE1 from β-clamp. As ImuB supports the association of ImuA′ and DnaE2, then induction of ImuB should trigger the transition from a high-fidelity to a low-fidelity replisome.

Together, our biochemical, structural, and computational results reinforce that the β-clamp is a central hub for DNA replication and mutagenesis, and therefore an attractive drug target for treatment of TB. Because the high-fidelity DnaE1 complex and the inducible low-fidelity DnaE2 mutasome engages the same binding pocket on the β-clamp, small molecules that block this interface should prevent all forms of DNA replication. The sub-micromolar affinity we measured for the ImuB motif (K_d ~ 0.9 μM) provides a quantitative benchmark for inhibitor design because partial inhibition could displace DnaE1 more readily than ImuB, paradoxically increasing mutation rates and accelerating drug resistance.

REFERENCES

1. Global tuberculosis report 2024. https://www.who.int/publications/i/item/9789240101531.
2. Mcgrath, M., Gey van pittius, N. C., Van helden, P. D., Warren, R. M. & Warner, D. F. Mutation rate and the emergence of drug resistance in Mycobacterium tuberculosis. Journal of Antimicrobial Chemotherapy 69, 292–302 (2014).
3. Wang, T.-C. & Chen, F.-C. The evolutionary landscape of the Mycobacterium tuberculosis genome. Gene 518, 187–193 (2013).
4. Reiche, M. A., Warner, D. F. & Mizrahi, V. Targeting DNA Replication and Repair for the Development of Novel Therapeutics against Tuberculosis. Frontiers in Molecular Biosciences 4, 1–18 (2017).
5. Altieri, A. S. & Kelman, Z. DNA sliding clamps as therapeutic targets. Frontiers in Molecular Biosciences 5, 87 (2018).
6. Wolff, P. et al. Structure-based design of short peptide ligands binding onto the E. coli processivity ring. J Med Chem 54, 4627–4637 (2011).
7. Bunting, K. A., Roe, S. M. & Pearl, L. H. Structural basis for recruitment of translesion DNA polymerase Pol IV/DinB to the beta-clamp. EMBO J 22, 5883–5892 (2003).
8. Timinskas, K., Balvočiūtė, M., Timinskas, A. & Venclovas, Č. Comprehensive analysis of DNA polymerase III α subunits and their homologs in bacterial genomes. Nucleic Acids Research 42, 1393–1413 (2014).
9. Baños-Mateos, S. et al. High-fidelity DNA replication in Mycobacterium tuberculosis relies on a trinuclear zinc center. Nature Communications 8, 855 (2017).
10. Rock, J. M. et al. DNA replication fidelity in Mycobacterium tuberculosis is mediated by an ancestral prokaryotic proofreader. Nature Genetics 47, 677–681 (2015).
11. Nasir, N. & Kisker, C. Mechanistic insights into the enzymatic activity and inhibition of the replicative polymerase exonuclease domain from Mycobacterium tuberculosis. DNA Repair (Amst) 74, 17–25 (2019).
12. Kling, A. et al. Targeting DnaN for tuberculosis therapy using novel griselimycins. Science 348, 1106–1112 (2015).
13. Warner, D. F. et al. Essential roles for imuA′- and imuB-encoded accessory factors in DnaE2-dependent mutagenesis in Mycobacterium tuberculosis. Proceedings of the National Academy of Sciences 107, 13093–13098 (2010).
14. Aragaw, W. W. et al. Cyclohexyl-griselimycin Is Active against Mycobacterium abscessus in Mice. Antimicrob Agents Chemother 66, e0140021 (2022).

15. Gui, W. J. et al. Crystal structure of DNA polymerase III β sliding clamp from Mycobacterium tuberculosis. Biochemical and Biophysical Research Communications 405, 272–277 (2011).
16. Emsley, P., Lohkamp, B., Scott, W. G. & Cowtan, K. Features and development of Coot. Acta Crystallogr D Biol Crystallogr 66, 486–501 (2010).
17. Huang, J., Lemkul, J. A., Eastman, P. K. & MacKerell, A. D. Molecular dynamics simulations using the drude polarizable force field on GPUs with OpenMM: Implementation, validation, and benchmarks. J Comput Chem 39, 1682–1689 (2018).
18. Wehmeyer, C. et al. Introduction to Markov state modeling with the PyEMMA software [Article v1.0]. Living Journal of Computational Molecular Science 1, 5965–5965 (2019).
19. Edwards, T. E., Liao, R., Phan, I., Myler, P. J. & Grundner, C. Mycobacterium thermoresistibile as a source of thermostable orthologs of Mycobacterium tuberculosis proteins. Protein Science 21, 1093–1096 (2012).
20. Vieille, C. & Zeikus, G. J. Hyperthermophilic enzymes: sources, uses, and molecular mechanisms for thermostability. Microbiol Mol Biol Rev 65, 1–43 (2001).
21. Hait, S., Mallik, S., Basu, S. & Kundu, S. Finding the generalized molecular principles of protein thermal stability. Proteins 88, 788–808 (2020).
22. Tina, K. G., Bhadra, R. & Srinivasan, N. PIC: Protein Interactions Calculator. Nucleic Acids Res 35, W473-476 (2007).
23. Ferruz, N., Schmidt, S. & Höcker, B. ProteinTools: a toolkit to analyze protein structures. Nucleic Acids Res 49, W559–W566 (2021).
24. Gallivan, J. P. & Dougherty, D. A. Cation-pi interactions in structural biology. Proc Natl Acad Sci U S A 96, 9459–9464 (1999).
25. Ditse, Z., Lamers, M. H. & Warner, D. F. DNA Replication in Mycobacterium tuberculosis. Microbiol Spectr 5, (2017).
26. Kana, B. D. et al. Role of the DinB homologs Rv1537 and Rv3056 in Mycobacterium tuberculosis. J Bacteriol 192, 2220–2227 (2010).
27. Dalrymple, B. P., Kongsuwan, K., Wijffels, G., Dixon, N. E. & Jennings, P. A. A universal protein-protein interaction motif in the eubacterial DNA replication and repair systems. Proc Natl Acad Sci U S A 98, 11627–11632 (2001).

ACKNOWLEDGMENTS

This work was supported internally by Iowa State University, including the College of Agriculture and Life Sciences and the Department of Veterinary Medicine.

AUTHOR CONTRIBUTIONS

M.K. performed all experiments except for the MD simulations, which were carried out by S.S. O.J.G. assisted M.K. with material generation. R.B.H. and S.W.N. conceived the project and wrote the manuscript along with M.K.. All authors have read and approved the final manuscript.

COMPETING INTERESTS

The authors declare that they have no competing interests.

SUPPLEMENTARY FIGURES

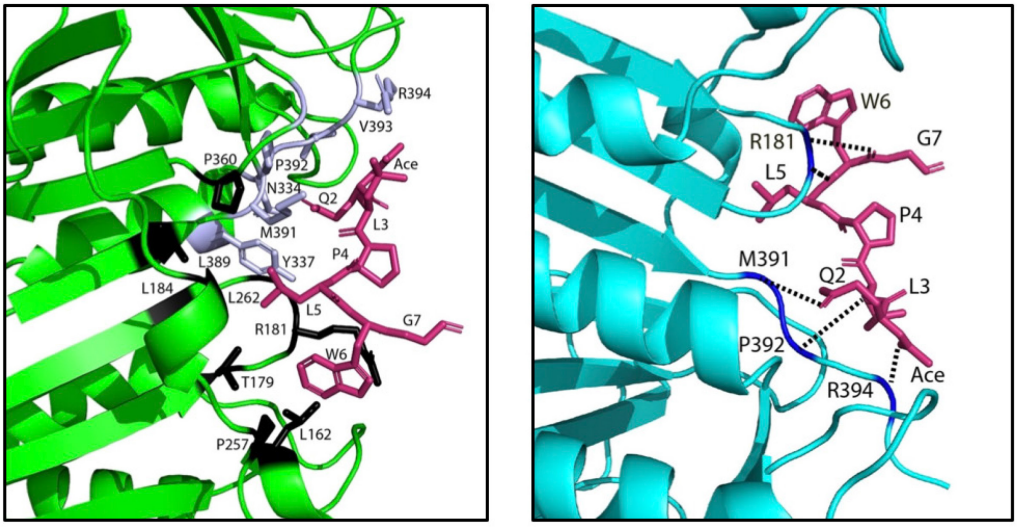

Figure S1. A) Orthogonal view of the binding site depicting hydrophobic residues in subsite I (black) and subsite II (purple). B) Binding pocket illustrating H-bond between the β-clamp residues (blue) and the ImuB peptide (pink).

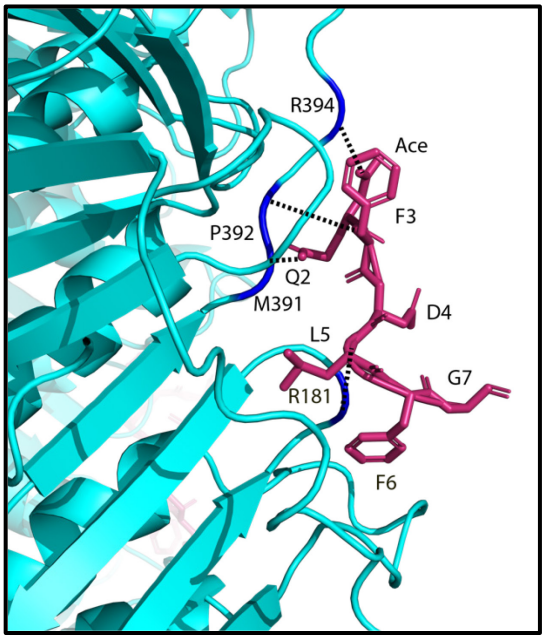

Figure S2. Orthogonal view of binding pocket illustrating H-bonds with the DnaE1 peptide

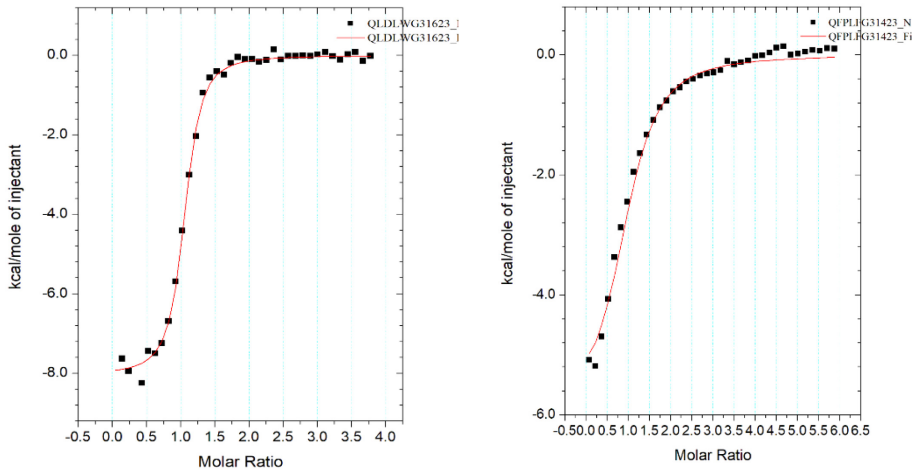

Figure S3. ITC of the interaction of β-clamp and ImuB P to D peptide and the DnaE1 D to P peptide at pH 8 at 25°C